RSC Advances

ROYAL SOCIETY OF CHEMISTRY

www.rsc.org/advances

Phase composition, crystal structure, complex chemical bond theory and microwave dielectric properties of high-Q materials in $(Nd_{1-x}Y_x)NbO_4$ system

Yonggui Zhao, Ping Zhang*

School of Electronic and Information Engineering and Key Laboratory of Advanced Ceramics and Machining Technology of Ministry of Education, Tianjin University, Tianjin 300072, P. R. China

Abstract

In this paper, the $(Nd_{1-x}Y_x)NbO_4$ ceramics are prepared via conventional solid-state reaction method and its microwave dielectric properties have been reported for the first time. The Rietveld refinement was used to investigate the crystal structure of $(Nd_{1-x}Y_x)NbO_4$ ceramics. Based on the refined results, the $NdNbO_4$ ceramics perform the monoclinic fergusonite structure (I2/a (15) space group, Z=4). The XRD patterns present a single monoclinic phase of $NdNbO_4$ in the range of x=0.02 to 0.1, with a further increase the substitution contents of Y^{3+} ions, little impurity phases are formed. In order to evaluate the correlations between complex chemical bond theory and microwave dielectric properties, the ionic polarization, lattice energy and bond energy were calculated using the refined lattice parameters and bond length. The effects of Y^{3+} ions substitution for Nd^{3+} ions on the microwave dielectric properties of $(Nd_{1-x}Y_x)NbO_4$ ceramics were also discussed. The increase in the dielectric constant ε_r is due to increasing corrected theoretical dielectric constant ε_{rc}. For the high relative density samples, the Q×f values and τ_f values are really dependence upon the calculated lattice energy and bond energy. High-quality factor microwave dielectric materials could be obtained with x=0.08 in the $(Nd_{1-x}Y_x)NbO_4$ system, and shown excellent dielectric properties of ε_r = 19.87, Q×f = 81,100 GHz and τ_f = -18.84 ppm/^{o}C.

*Corresponding author. Tel. : +86 13702194791

Email address: zptai@163.com (P. Zhang)

Key words: High-Q ceramics; Crystal structure; Rietveld refinement; Lattice energy; Bond energy;

1. Introduction

Remands for wireless industry with a wide range of applications from microwave communication to intelligent transport systems have led to development of low loss, high relative permittivity and near zero temperature coefficients of resonant frequency ceramics receiving more attentions than ever. Microwave dielectrics materials with high performance and the structure property have always attracted considerable attention. Therefore, numbers microwave dielectric materials are being developed to meet the requirements for small-sized and better selectivity GPS patch antennas in the last few years [1-4].

Recently, numbers researches have focused on the microwave dielectric materials of ABO_4 compounds due to the flexibility in substituting different elements at the A- and B-site, which could lead to optimum microwave dielectric properties [5-7]. When the A- and B-site were substituted by lanthanoid and niobium elements, respectively, a new ABO_4 composition materials system of rare-earth orthoniobates materials system $RENbO_4$ (RE=lanthanoid atoms, being La to Lu as well as Y) is developed. The $RENbO_4$ materials have similar fergusonite-type structure (monoclinic, $C_{2/C}$) and properties, which are firstly studied on the luminescence characteristic, damping characteristic and phase transformation characteristic [8-11].

When the RE=Nd, the $NdNbO_4$ composition system is developed. The microwave dielectric properties of $NdNbO_4$ ceramics with ε_r=19.6, $Q\times f$= 33, 000 GHz and τ_f= -24ppm/^oC was firstly reported by *Kim, et al* [12]. In the recent years, numbers researches on the microwave dielectric properties have been carried out [13-20]. For example, *Zhang et al*. [13] have studied the effects of CaF_2, $CaTiO_3$ and CuO additives on the microwave dielectric properties and sintering behavior of

$NdNbO_4$ ceramics. The $NdNbO_4$ ceramics with 2.0 wt.% CaF_2 sintered at 1225 ^oC for 4h shows excellent microwave dielectric properties, $Q\times f$ ~75, 000 GHz and τ_f ~ -19 ppm/ ^oC. With the increasing of the $CaTiO_3$ contents additions, the $NdNbO_4$-$CaTiO_3$ system has a trend of shifting toward zero in the whole range for the τ_f values [14]. Moreover, a high $Q\times f$ value of 70, 000 GHz with 0.6 wt.% $CaTiO_3$ additive could be obtained sintered at 1275 ^oC for 4 h. The effects of CuO addition on the sintering properties of $NdNbO_4$ were also studied, the sintering temperature of $NdNbO_4$ can be lowered to 975 ^oC doped with 0.2 wt. % CuO addition, and the microwave dielectric properties of $NdNbO_4$ were not affected apparently [15]. Recently, *Zhang et al.* discovered that the microwave properties of $NdNbO_4$ ceramics could be optimized using bivalent ions substituted to Nd^{3+}ionic owing to formation of solid solutions and the phase composition would be changed when Nd^{3+} ionic was substituted by bivalent ions (Sr^{2+}, Ca^{2+}, Mn^{2+}, Co^{2+}) [16-17]. The effects of Ta^{5+} and Sb^{5+} ions substitution for the $NdNbO_4$ ceramics were also investigated, a small level of Sb^{5+} substitution (x= 0.06) could greatly improve the $Q\times f$ values for the $NdNbO_4$ ceramics [18-20]. And the phase change was also investigated and that proved to play an important role on $NdNbO_4$ ceramics. However, few works were reported about the effects of trivalent ions (especially the lanthanoid ions) substitution for Nd^3+ ions on the microwave properties of $NdNbO_4$ ceramics. And a high quality factor and the crystal structure of $NdNbO_4$ ceramics using trivalent ions substitution have not been discussed. Moreover, the effects of Y^{3+} ion substitution for Nd^{3+} on the ionic polarization, oxygen octahedral distortion, lattice energy and bond energy in $NdNbO_4$ system were also not investigated.

In this paper, $(Nd_{1-x}Y_x)NbO_4$ ($0.02\leq x\leq 0.15$) ceramics were prepared to study the influence of Y^{3+} ions substitution on the phase evolution, octahedral distortion, lattice energy, bond energy and microwave dielectric properties. The lattice energy and bond energy were calculated based on the

complex chemical bond theory to develop a relationship between the theoretical calculations and the microwave dielectric properties. Moreover, an available method based on the Rietveld refinement of X-ray techniques was used to analyze the crystal structure.

2. Experimental procedure

The $(Nd_{1-x}Y_x)NbO_4$ (x=0.02-0.15) compounds were prepared by a conventional solid-state reaction method. The Nd_2O_3, Y_2O_3, and Nb_2O_5 (High-Purity Chemicals 99.9%) were used as raw materials. Stoichiometric mixtures of starting materials were ball-milled with distilled water for 6 h. All the slurries were dried, crushed and sieved with a 40 mesh screen. Then the sieved specimens calcined at 900 °C for 4 h, the obtained powders were re-milled for 6 h. After drying, the crushed powders sieved with a 40 mesh screen firstly, then granulated doping with 6 wt% paraffin as a binder and sieved with an 80 mesh screen, the powders were pressed into disk-typepellets with 10 mm diameter and 5 mm thickness at 100 MPa. Then these pellets were sintered at temperatures of 1225 - 1275 ^oC for 4 h in air with the heating rate of 5 ^oC/min based on the previous process conditions [14-18].

The crystal structures of the synthesized samples were identified by X-ray diffraction (XRD, Rigaku D/max 2550 PC, Tokyo, Japan) with Cu Kα radiation generated at 40 kV and 40 mA. The microstructure of the ceramic surfaces were performed and analyzed by a scanning electron microscopy (SEM, MERLIN Compact, Germany). The microwave dielectric properties were measured in the frequency range of 8-12 GHz using a HP8720ES network analyzer. The temperature coefficients of resonant frequency (τ_f) were measured in the temperature range from 25 °C to 85 °C. The τ_f (ppm/ °C) was calculated by noting the change in resonant frequency (Δf)

$$\tau_f = \frac{f_{85} - f_{25}}{f_{25}(85-25)} \quad (1)$$

where f_{25} is resonant frequency at 25^oC and f_{85} is the resonant frequency at 85^oC.

The apparent densities of the sintered pellets were measured use the Archimedes method (Mettler ToledoXS64). To study the relative density of the sample, the theoretical density was obtained from the crystal structure and atomic weight by the Eq. (2):

$$\rho_{theory} = \frac{ZA}{V_C N_A} \quad (2)$$

where V_C, N_A , Z, and A are volume of unit cell (cm^3), avogadro number (mol^{-1}), number of atoms in unit cell, and atomic weight (g/mol), respectively. The relative density was obtained by the Eq. (3):

$$\rho_{relative} = \frac{\rho_{bulk}}{\rho_{theory}} \times 100\% \quad (3)$$

3. Results and discussion

3.1Multiphase refinement

Fig.1 shows the XRD patterns of $(Nd_{1-x}Y_x)NbO_4$ (x=0.02-0.15) ceramics sintered at 1250°C for 4 h. All of the peaks were clearly indexed as the monoclinic phase for $NdNbO_4$ (PDF. No. 32-0680) in the range of x=0.02 to 0.10. As the x value increases to 0.15, some impurity phases can be observed. The formation of the impurity phase would be due to reaction of the exceed Y^{3+} ionic with the Nb^{5+} ionic which indicates the solid solution of the $(Nd_{1-x}Y_x)NbO_4$ is lower than 0.15. In order to clarify the effects of Y^{3+} ionic substitution for Nd^{3+} ionic on the crystal structure of $(Nd_{1-x}Y_x)NbO_4$ ceramics, the refinements were performed using Full-prof software based on X-ray diffraction data of the $(Nd_{1-x}Y_x)NbO_4$ (x=0.02-0.15) samples. And the refined lattice parameters, cell volume, reliability factors, bond length and atomic coordinate information were presented in Table. 1-2. In addition, the structural refinement patterns of the $(Nd_{0.92}Y_{0.08})NbO_4$ ceramic are offered in Fig. 2. According to the Rietveld refinement results, the lattice parameters for $(Nd_{0.92}Y_{0.08})NbO_4$ ceramic are calculated as a=5.434 Å, b=11.229 Å, c=5.134 Å, β=94.40° and V=312.37 $Å^3$, the Rietveld discrepancy factors R_p and R_{wp} are 12.00 % and 12.90 %. As Table.1 shows, the lattice parameters and cell volumes slightly

decrease with increased Y^{3+} ionic content in the range of x=0.02-0.08, which is due to the incorporation of smaller Y^{3+}(1.019 Å, CN =8) in place of Nd^{3+}(1.109 Å, CN = 8) [21]. Therefore, the substitution of Y^{3+} ionic for Nd^{3+} ionic could decrease the unit cell volume of $NdNbO_4$. When the x value increase to 0.10, increase tendency in the lattice parameters is observed, which indicates that there could have an abnormal change in the crystal structure for the $NdNbO_4$ and the second phase was formed.

3.2 Crystal structure analysis

The schematic crystal structures of monoclinic fergusonite structure for $(Nd_{0.92}Y_{0.08})NbO_4$ ceramic are shown in Fig.3. There contains four $NdNbO_4$ molecules per primitive cell, and the Nb^{5+} ions are connected with six oxygen atoms forming distorted NbO_6 octahedron. Three Nb-site octahedrons by edge sharing are formed a "V" type arrangement. In the monoclinic fergusonite structure, Nd^{3+} and Nb^{5+} occupy 4e Wyckoff positions whereas the two distinguishable oxygen atoms occupy the same positions 8f named O1 and O2. As Fig. 3 shows, O1 atoms are connected with two Nd atoms and two Nb atoms, and the O2 atoms are connected with two Nd atoms and one Nb atom. In this paper, with the increasing of Y^{3+} ions contents, the atomic interactions of $NdNbO_4$ ceramics would be changed, which could result in the oxygen octahedron distortion. The change of the oxygen octahedron distortion has close connection with the lattice energy and bond energy, which as intrinsic factors to affect the microwave dielectric properties. Fig.4 presents the variation tendency of Nb-site octahedron distortion. In order to investigate the influence of Y^{3+} substitution on the interaction of the oxygen octahedron distortion accuracy, the calculation for the bond strength to introduce in this paper firstly, which calculated from follows formula [22]:

$$S = (\frac{R}{R_1})^{-N} \quad \text{or} \quad S = e^{-(\frac{R-R_0}{B})} \tag{4}$$

where R is the refined bond length shown in Table.1, R_1=2.137, N=6.5 for Nd-site and R_1=1.907, N=5

for Nb-site are the universal bond-strength-bond-length parameters from Ref 22. The details of bond strength for the $(Nd_{1-x}Y_x)NbO_4$ (x=0.02-0.15) ceramics are given in Table.3. Notice that the Nb-site octahedron has higher bond strength than the Nd-site, which suggests that the Nb-site octahedron distortion has more contribution to the microwave dielectric properties of the $NdNbO_4$ ceramic. The variation of the Nb-site bond strength with difference substitution ions are given in Fig.5. Obvious conclusions can be observed from the Fig.5, with the x values increase from 0.02 to 0.15, the Nb-site bond strength keeps an increasing tendency which indicates the decrease in Nb-site octahedron distortion. Stable Nb-site oxygen octahedron system could be obtained for $(Nd_{0.85}Y_{0.15})NbO_4$ ceramic.

3.3. Microstructure analysis

Figure.6 presents the SEM images of the compounds using $(Nd_{1-x}Y_x)NbO_4$ (x=0.02-0.15) ceramics sintered at 1250 ^oC for 4h. The results indicate that well-developed microstructures and nearly full densification of $(Nd_{1-x}Y_x)NbO_4$ ceramics can be achieved at suitable x value. The increase of sintering temperature helped to promote the grain growth, and a relative increase in the grain size was achieved for specimen shown in Fig.6 (a)-(d). The optimum microstructure could be achieved at x=0.08 in Fig.6 (d) which performed homogeneous grains and smooth surface. Moreover, all the estimated mean particle size was in the range of 3-5 μm. However, with a further increase in x values from 0.10 to 0.15 would result in a decreased tend in grain size and some pores, which cause the low relative densities of the specimens, as illustrated in Fig. 6(e)-(f).

3.4. Microwave dielectric properties analysis

Fig.7 shows the relative density, dielectric constant and quality factor of $(Nd_{1-x}Y_x)NbO_4$ (x=0.02-0.15) ceramics with different sintering temperature. As sintering temperature varied from 1225^{o}C to 1275 ^{o}C, both of the relative density and dielectric constant increase and reach a saturated

value, which is due to that high relative density means low pores (ε_r=1). And a higher dielectric constant with high relative density for $(Nd_{1-x}Y_x)NbO_4$ (x=0.02-0.15) ceramics could be obtained sintered at 1250^{o}C for 4h. The quality factor also presents a closely relationship with the sintering temperature because the extrinsic dielectric loss of the microwave dielectric ceramics are determined by the universal defects caused by the porosity, grain boundary, etc. The optimized sintering process, especially the sintering temperature could help to decrease the extrinsic dielectric loss and enhance the $Q\times f$ values. In this paper, the sintering time and heating rate based on our previous work are not under consideration in investigates the influence factors for the $Q\times f$ values. Observe that the $Q\times f$ values of the sintered specimens increased firstly with sintering temperature and then decreased, which indicated that an appropriate sintering temperature can help to enhance the $Q\times f$ values.

The microwave dielectric properties of $(Nd_{1-x}Y_x)NbO_4$ (x=0.02-0.15) ceramics sintered at the optimal sintering temperature are presented in Fig.8. Our recent works demonstrated that the microwave dielectric properties of sintered ceramics possessed high relative density have no obvious relationship with the extrinsic factors like the sintering temperatures, grain boundary and pores [23-26]. In this paper, the dielectric constant of $(Nd_{1-x}Y_x)NbO_4$ (x=0.02-0.15) ceramics at the optimal sintering temperature is dependence on the dielectric polarizabilities, and have vital effects to the theoretical dielectric constant. In order to clarify the effects of Y^{3+} substitution for Nd^{3+} on the dielectric constant, the theoretical dielectric constant ε_{rt} was calculated based on the Clausiuse- Mosotti equation [27] using the ionic polarizabilities, which was described as:

$$\alpha_D = \frac{V_m(\varepsilon_{rt}-1)}{b(\varepsilon_{rt}+2)} \quad (5)$$

$$\varepsilon_{rt} = \frac{(V_m+2b\alpha_D)}{(V_m-b\alpha_D)} \quad (6)$$

After considering the influence of porosity, the theoretical dielectric constant ε_{rt} was corrected as

follows [28]:

$$\varepsilon_{rc} = \varepsilon_{rt}\left(1 - \frac{3P(\varepsilon_{tr} - 1)}{2\varepsilon_{tr} + 1}\right) \quad (7)$$

where ε_{rt} is the theoretical dielectric constant; ε_{rc} is the corrected theoretical dielectric constant; V_m is the molar volume; α_D is the theoretical dielectric polarizability; b has the value of $4\pi/3$; P is the fractional porosity. Based on the additivity rule of molecular polarizabilities, the molecular polarizability of a complex substance (like $(Nd_{1-x}Y_x)NbO_4$) can be broken up into the molecular polarizabilities of simper substances states:

$$\alpha_D((Nd_{1-x}Y_x)NbO_4)=(1-x)\alpha_D(Nd^{3+})+x\alpha_D(Y^{3+})+\alpha_D(Nb^{5+})+4\alpha_D(O^{2-}) \quad (8)$$

Table.4 shows the change of the corrected theoretical dielectric constant (ε_{rc}) and the molecular polarizability (α_D) of the $(Nd_{1-x}Y_x)NbO_4$ compounds at optimal sintering temperature. With the increasing of x values, both of the ε_{rc} and α_D have an increasing tendency, which indicates the substitutions Y^{3+} ions for Nd^{3+} ions could enhance the polarizability of the $NdNbO_4$ ceramics. According to the calculation results, the variation of the experimental dielectric constant ε_r as a function of the corrected theoretical dielectric constant ε_{rc} is presented in Fig. 8(a). Notice that the ε_r and ε_{rc} present the similar variation tendency, which suggests that the ε_{rc} could predict the variation of the experimental dielectric constant ε_r when the specimens possess high relative density.

Fig.8 (b) shows the $Q\times f$ values for $(Nd_{1-x}Y_x)NbO_4$ with different substitution contents sintered at the optimal sintering temperature. As we all known, the $Q\times f$ values were affected by many factors, and it can be divided into two fields, the intrinsic loss and extrinsic loss. In this paper, the effect of extrinsic loss like the second phases, oxygen vacancies, grain boundaries, and densification or porosity is minimal to the $Q\times f$ values due to the high densified compounds. In the previous work, the $Q\times f$ values

with oxygen octahedron structure are observed to relate to the lattice energy [19, 29, and 30]. Based on the generalized P-V-L theory [31], the lattice energy for the single-bond crystal was consisted of the ionic and covalent parts. The ionic part mainly results from electrostatic interactions and repulsive interactions of the ion pairs, and another arises from the overlap of electron clouds. With an increase in the lattice energy, the Q×*f* values would increase. And the lattice energy U_{cal} of a complex crystal can be calculated as follows:

$$U_{cal} = \sum_{\mu} U_b \tag{9}$$

For any binary crystal A_mB_n type compounds, the lattice energy U_b is described as:

$$U_b = U_{bc} + U_{bi} \tag{10}$$

$$U_{bc} = 2100m\frac{(Z_+)^{1.64}}{(d)^{0.75}} f_c \tag{11}$$

$$U_{bi} = 1270\frac{(m+n)Z_+Z_-}{d}(1-\frac{0.4}{d}) f_i \tag{12}$$

where U_{bc} is the covalent part and U_{bi} is the ionic part of bond type A-B; d was the distance between the cation A and anion B; m and n were the numbers of cation A and anion B; Z_+ and Z_- are the valence states of cation and anion which constituted to the bond type A-B; f_i and f_c are the bond ionicity and bond covalenc, which could be obtained from ref.19. The calculated lattice energy for $(Nd_{1-x}Y_x)NbO_4$ (x=0.02-0.15) ceramics sintered at 1250°C is illustrated in Table.5. Fig. 8 (b) presents the variation of Q×*f* values as a function of the Nd-site lattice energy. With the Y^{3+} ions contents increased, the lattice energy increased which led to an increase in the Q×*f* values. This phenomenon is because that the Q×*f* values are mainly decided by the lattice anharmonicity, and when the lattice energy increased, the lattice anharmonicity would be enhanced which would decrease the intrinsic loss, therefore, the Q×*f* value would increase.

As we all known, usually shorter bond length correlates with higher bond energy, and higher bond

energy suggests more stable system. Our recent work suggests that the bond energy can affect the temperature coefficient of resonant frequency τ_f values, and higher bond energy correlates a smaller $|\tau_f|$ value [20, 29]. The bond energy E of a complex crystal could be written as:

$$E = \sum_{\mu} E_b^{\mu} \tag{13}$$

where E_b^{μ} is bond energy for the type μ bond, which is composed of nonpolar covalence energy E_c^{μ} and complete ionicity energy E_i^{μ} parts as follows:

$$E_b^{\mu} = t_c E_c^{\mu} + t_i E_i^{\mu} \tag{14}$$

The energy of the ionic form E_i^{μ} was the unit charge product divided by the bond length d^{μ}, adjusted to kcal/ mol by the factor 33200 when the bond length is pm.

$$E_i^{\mu} = \frac{33200}{d^{\mu}} \tag{15}$$

For any binary crystal A_mB_n type compounds, the nonpolar covalence energy E_c^{μ} parts could be calculated as following:

$$E_c^{\mu} = \frac{(r_{cA} + r_{cB})}{d^{\mu}} (E_{A-A} E_{B-B})^{1/2} \tag{16}$$

where r_{cA} and r_{cB} are the covalent radii, $E_{A\text{-}A}$ and $E_{B\text{-}B}$ were the homonuclear bond energy, which can be obtained from the handbook of bond energies [32]. In this paper, $E_{Nd\text{-}Nd}$=82.8 kJ/mol, $E_{Y\text{-}Y}$=270 kJ/mol, $E_{Nb\text{-}Nb}$=513 kJ/mol, and $E_{O\text{-}O}$=498.36 kJ/mol; r_{cNd}=174 pm, r_{cY}=163 pm, r_{cNb}=147 pm and r_{cO}= 63 pm.

For the Eq. (14), t_c and t_i are the covalent and ionic blending coefficients, respectively. The relationship of t_c and t_i can be described by the following formula:

$$t_c + t_i = 1 \tag{17}$$

The ionic blending coefficient t_i is defined as:

$$t_i = \left| \frac{(S_A - S_B)/\Delta S_B}{2} \right| \tag{18}$$

where S_A and S_B are the electronegativities of A and B ions. ΔS_B is the change for complete of an electron. In this paper, S_{Nd}=1.14, S_Y=1.22, S_{Nb}=1.59, S_O=3.44 and $\Delta S_B = \Delta S_O$=3. The details of bond energy are given in Table. 6-7. Fig.8 (c) shows the τ_f values of $(Nd_{1-x}Y_x)NbO_4$ ceramics (x=0.02 to 0.08) as a function of bond energy. The variation of τ_f values is consistent with the bond energy. With the increase of the bond energy, the $|\tau_f|$ values decreased. That's because with the increasing of the bond energy the distortion of oxygen octahedral would be recovered, and the τ_f values have close relationship with the distortion of oxygen octahedral. Therefore, higher bond energy would recover the distortion of oxygen octahedral which correlates a smaller $|\tau_f|$ value. As the x values increase to 0.10, the second phase is formed, which have vital effects on the τ_f values. Therefore, the increasing tendency of $|\tau_f|$ value in Table.8 could be attributed to the formation of the second phase.

Table.8 shows the relative density, ε_r values, $Q \times f$ values and τ_f values for the $(Nd_{1-x}Y_x)NbO_4$ samples with different x values sintered at optimal sintering temperature. When x=0.08, excellent microwave dielectric properties with a ε_r value of 19.87, a very high $Q \times f$ value of 81,100 GHz and τ_f value of -18.84 ppm/°C could be obtained.

4. Conclusions

The phase composition, lattice energy, bond energy and microwave dielectric properties of $(Nd_{1-x}Y_x)NbO_4$ (x=0.02-0.15) ceramics were investigated in present study. The Rietveld refinement revealed that $NdNbO_4$ ceramics performed the monoclinic fergusonite structure and possessed an Nb-site oxygen octahedron. With the increasing of the x values, the oxygen octahedron distortion, which c characterized by the Nb-site bond strength, would decrease. In order to demonstrate the intrinsic factors for the microwave dielectric properties, theoretical calculation based on the complex chemical bond theory was introduced in this paper. The calculated results indicates that the ε_r, $Q \times f$

value and τ_f value for the $(Nd_{1-x}Y_x)NbO_4$ ceramics with high relative density are mainly dependent on the dielectric polarizabilities, lattice energy and bond energy, respectively. The change of the Y^{3+} contents have obvious effect on the microwave dielectric properties of $(Nd_{1-x}Y_x)NbO_4$ ceramics which is due to the difference of the Y^{3+} and Nd^{3+} in the polarizabilities, electronegativities, and bond energy, etc. At 1250°C, the $(Nd_{1-x}Y_x)NbO_4$ ceramics with x=0.08 possesses excellent microwave dielectric properties with an ε_r value of 19.87, a high $Q \times f$ value of 81,100 GHz and τ_f value of -18.84 ppm/°C.

Acknowledgments

The authors gratefully acknowledged supports from the Key Laboratory of Advanced Ceramics and Machining Technology, Ministry of Education (Tianjin University). The author would like to thank Hai-Tao Wu for his help in XRD experiments.

References

1. M. T. Sebastian, Dielectric materials for wireless communication, Elsevier publishing group, 2008.

2. S. D. Ramarao and V. R. K. Murthy, *Dalton. Trans*., 2015, 44, 2311.

3. S. D. Ramarao and V. R. K. Murthy, *Phys. Chem. Chem. Phys*., 2015, 17, 12623.

4. D. Zhou, B. W. Li, H. H. Xi, L. X. Pang and G. S. Pang, *J. Mater. Chem. C*., 2015, 3, 2582.

5. S. H. Yoon, D. W. Kim, S. Y. Cho and K. S. Hong, *J. Eur. Ceram. Soc*., 2006, 26, 2051.

6. R. C. Pullar, S. Farrah and N. M. Alford, *J. Eur. Ceram. Soc*., 2007, 27, 1059.

7. E. S. Kim, B. S. Chun, R. Freer and R. J. Cernik, *J. Eur. Ceram. Soc*., 2010, 30, 1731.

8. L. H. Brixner, J. F. Whitney, F. C. Zumsteg, G. A. Jones, *Mat. Res. Bull*., 1997, 12, 17.

9. S. K. Lee, H. Chang, C. H. Han, H. J. Kim, *J. Solid. State. Chem*., 2001, 156, 267.

10. K. Nishiyama, T. Abe , T. Sakaguchi , N. Momozawa, *J. Alloy. Compd*., 2003, 355, 103.

11. J. Li and C. M. Wayman, *J. Am. Ceram. Soc*., 1997, 80, 803.

12. D. W. Kim, D. K. Kwon, S. H. Yoon, K. S. Hong, *J. Am. Ceram. Soc*., 2006, 89, 3861.

13. P. Zhang, T. Wang, W. S. Xia, L. X. Li, *J. Alloy. Compd*., 2012, 535, 1.

14. P. Zhang, Z. K. Song, Y. Wang, Y. M. Han, H. L. Dong, L. X. Li, *J. Alloy. Compd*., 2013, 581, 741.

15. P. Zhang, Z. K. Song, B. L. Gao, Y. Wang, T. Wang, Y. M. Han, *Mater. Res. Innov*., 2014, 18, 284.

16. P. Zhang, Z. K. Song, Y. Wang, L. X. Li. *J. Am. Ceram. Soc*., 2014, 97, 976.

17. Z. K. Song, P. Zhang, Y. Wang, L. X. Li. *J. Alloy. Compd*., 2014, 583, 546.

18. P. Zhang, Y. G. Zhao, J. Liu, Z. K. Song, M. Xiao, X. Y. Wang, *Dalton. Trans*., 2015, 44, 5053.

19. P. Zhang, Y. G. Zhao, X. Y. Wang, *Dalton. Trans*., 2015, 44, 10932

20. P. Zhang, Y. G. Zhao, X. Y. Wang, *J. Alloy. Compd*., 2014, 644, 621.

21. R. D. Shannon, *Acta. Crystallogr*., 1976, A32, 751.

22. I. D. Brown, R. D. Shannon, *Acta. Crystallogr*., 1973, 29, 266.

23. D. Zhou, W. B. Li, L. X. Pang, Z. X. Yue, G. S. Pang and X. Yao, RSC. Adv., 2015, 5,19255.

24. W. S. Kim, K. H. Yoon, E. S. Kim., *J. Am. Ceram. Soc*., 83 (2000) 2327-2329.

25. E. S. Kim, B. S. Chun, R. Freer, R. J. Cernik, *J. Eur. Ceram. Soc*., 2010, 30, 1731.

26. W. S. Xia, L. X. Li, P. F. Ning, Q. W. Liao, *J. Am. Ceram. Soc*., 2012, 95(8), 1.

27. R. D. Shannon, *J. Appl. Phys*., 73, 1993, 348.

28. W. R. Yang, P. Z. Huang, C. L. Huang, *J. Alloy. Compd*., 2015, 620, 18.

29 P. Zhang, Y. G. Zhao, X. Y. Wang, *J. Alloy. Compd*., 2015, 654, 240.

30. P. Zhang, Y. G. Zhao, H. T. Wu, *Dalton. Trans*., 2015, 44, 16684.

31. D. T. Liu, S. Y. Zhang, Z. J. Wu, *Inorg. Chem*., 2003, 42, 2465.

32. Y. R. Luo, Comprehensive Handbook of Chemical Bond Energies., CRC Press 2007.

Figure captions

Fig.1 The XRD patterns of $(Nd_{1-x}Y_x)$ NbO_4 ceramics with different x values sintered at 1250 °C for 4h.

Fig.2 The structural refinement patterns of the $(Nd_{0.92}Y_{0.08})NbO_4$ ceramic.

Fig.3 The crystal structure patterns (1 × 1 × 1) supercell of monoclinic fergusonite structured $(Nd_{0.92}Y_{0.08})NbO_4$.

Fig.4 Distortion in BO_6 for $(Nd_{1-x}Y_x)$ NbO_4 (a) x=0.02; (b) x=0.08; (c) x=0.15.

Fig.5 The Nb-site bond strength for $(Nd_{1-x}Y_x)$ NbO_4 as a function of x values.

Fig.6. The SEM micrographs for $(Nd_{1-x}Y_x)NbO_4$ ceramics sintered at 1250 °C for 4 h with (a) x=0.02, (b) x=0.04, (c) x=0.06, (d) x=0.08, (e) x=0.10, (f) x=0.15.

Fig.7 (a) Relative densities and ε_r values of $(Nd_{1-x}Y_x)$ NbO_4 ceramics with x=0.02-0.15 at different sintering temperature; (b) Q×f values of $(Nd_{1-x}Y_x)NbO_4$ ceramics with x=0.02-0.15 at different sintering temperature.

Fig.8 (a) The corrected theoretical dielectric constants ε_{rc} and experimental dielectric constants ε_r of $(Nd_{1-x}Y_x)NbO_4$ ceramics with x=0.02-0.15; (b) The Q×f values of $(Nd_{1-x}Y_x)NbO_4$ ceramics with x=0.02-0.15 as a function of Nd-site lattice energy; (c) The τ_f values of $(Nd_{1-x}Y_x)NbO_4$ ceramics with x=0.02-0.08 as a function of bond energy.

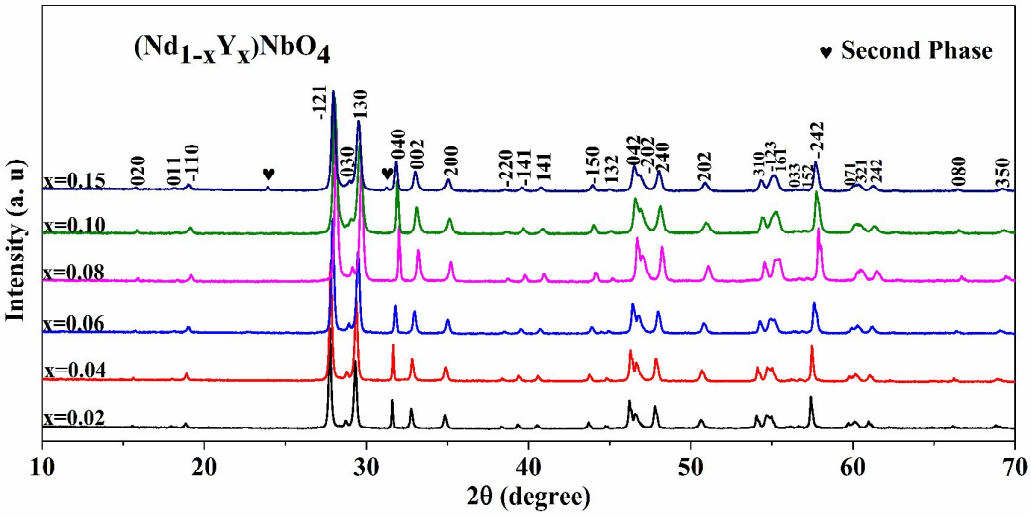

Fig. 1

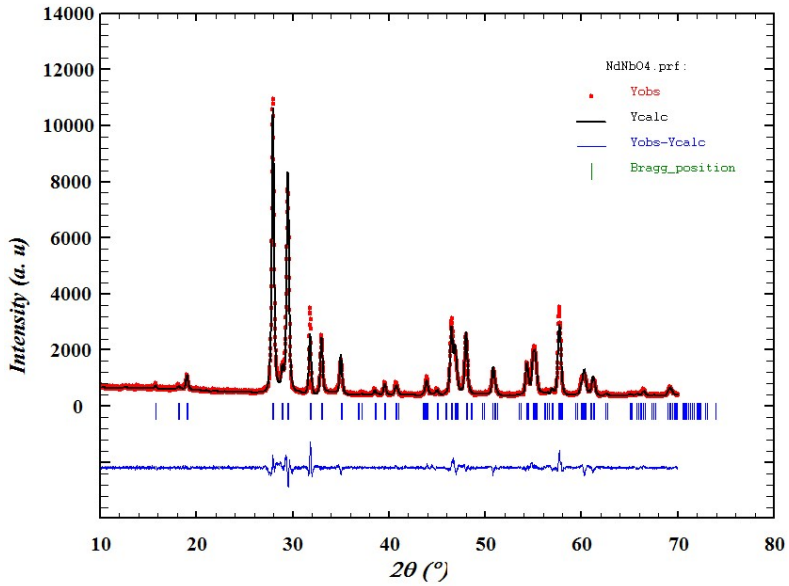

Fig.2

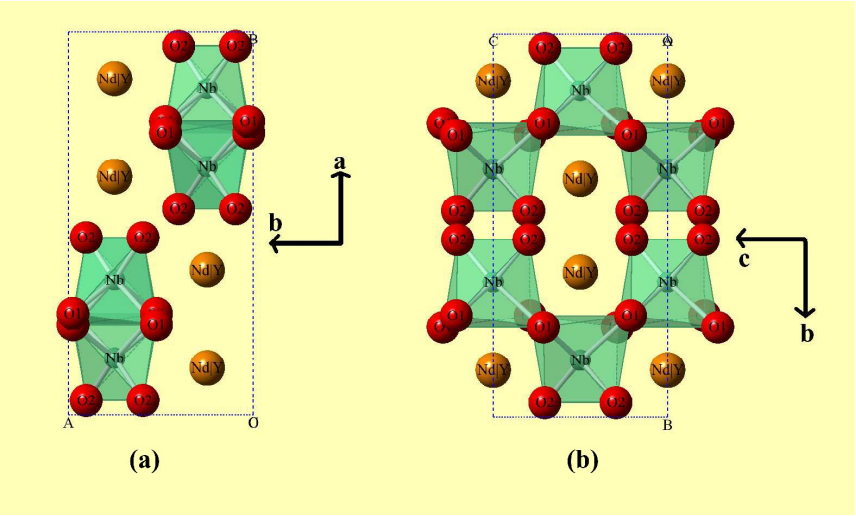

Fig.3

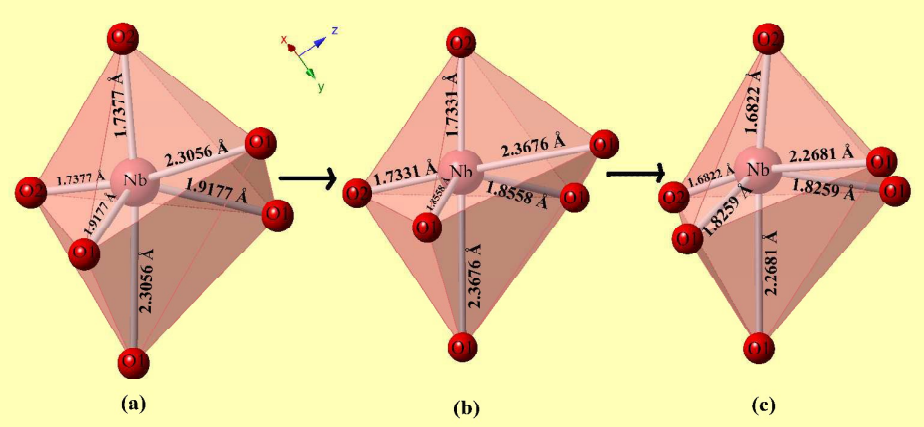

Fig.4

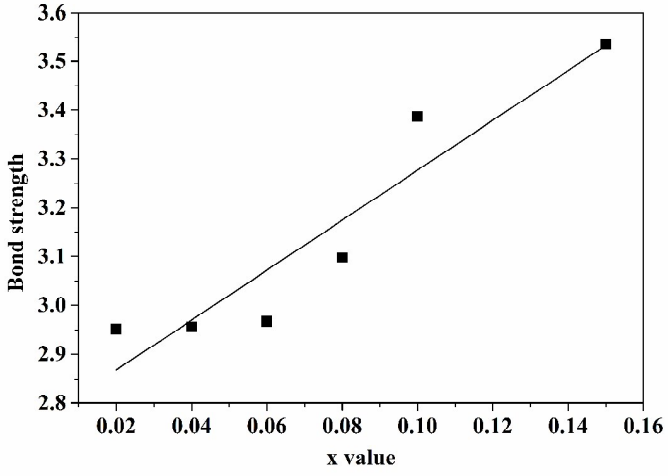

Fig.5

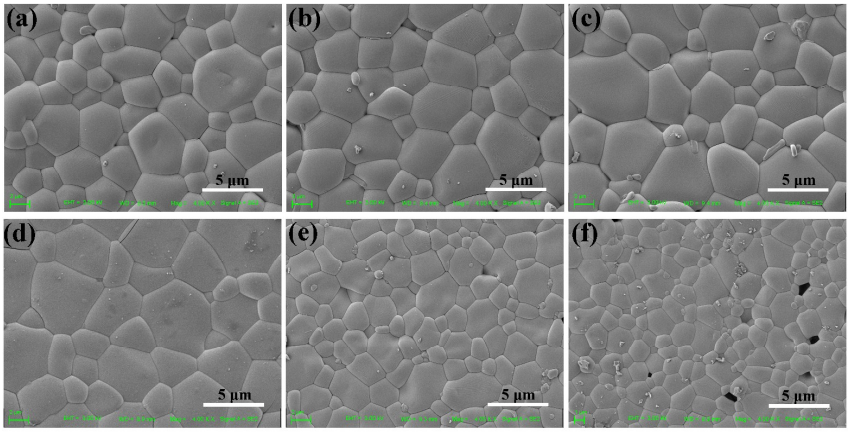

Fig. 6

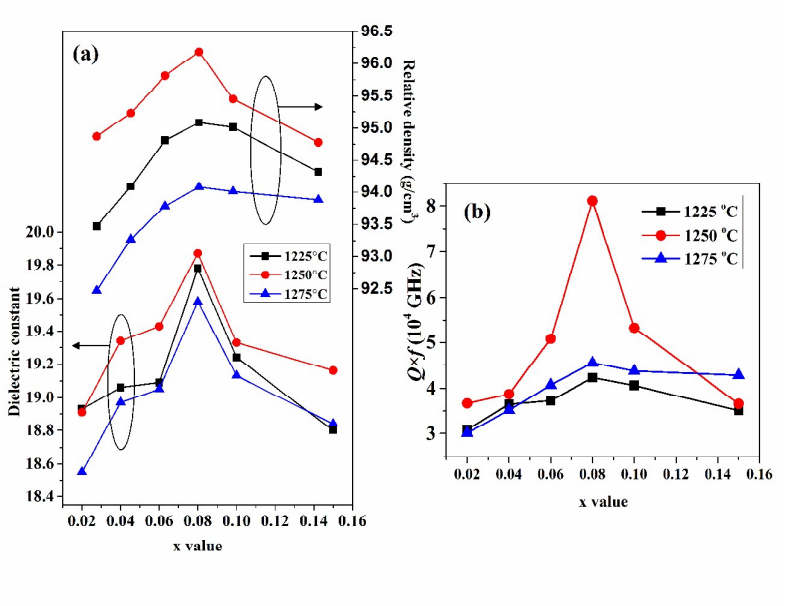

Fig. 7

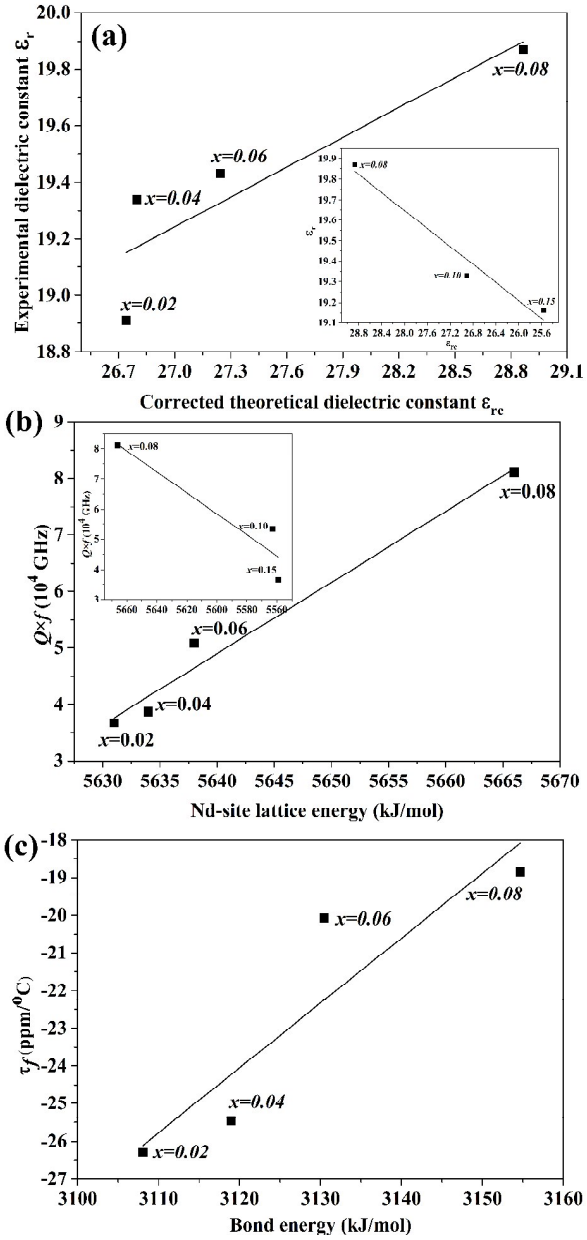

Fig. 8

Table.1 Refined lattice parameters, cell volume ($Å^3$), reliability factors and bond length of $(Nd_{1-x}Y_x)NbO_4$ ceramics with x=0.02-0.15 sintered at 1250 °C for 4h.

x value	*x=0.02*	*x=0.04*	*x=0.06*	*x=0.08*	*x=0.10*	*x=0.15*
a	5.457	5.454	5.449	5.434	5.442	5.443
b	11.271	11.267	11.257	11.229	11.251	11.252
c	5.144	5.143	5.141	5.134	5.139	5.141
β	94.44	94.43	94.42	94.40	94.38	94.36
V_{cell}	315.45	315.11	314.42	312.37	313.75	313.97
R_p	0.0638	0.0644	0.1190	0.1200	0.1430	0.1430
R_{wp}	0.0911	0.0985	0.1260	0.1290	0.1560	0.1500
Nd/Y-O(1)[1](Å) ×2	2.4848	2.4838	2.4818	2.4362	2.5402	2.5201
Nd/Y-O(1)[2](Å) ×2	2.5380	2.5370	2.5352	2.5461	2.6782	2.7151
Nd/Y-O(2)[1](Å) ×2	2.4290	2.4282	2.4266	2.4117	2.3628	2.3160
Nd/Y-O(2)[2](Å) ×2	2.6172	2.6163	2.6143	2.6058	2.6572	2.7092
Nb-O(1)[1](Å)×2	1.9177	1.9169	1.9154	1.8558	1.8248	1.8259
Nb-O(1)[2](Å) ×2	2.3056	2.3049	2.3034	2.3676	2.2620	2.2681
Nb-O(2)(Å) ×2	1.7377	1.7372	1.7360	1.7331	1.7122	1.6822

Table.2 Refined Atomic Fractional Coordinates from XRD data for $(Nd_{0.92}Y_{0.08})NbO_4$.

Element	*Wyckoff site*	*x*	*y*	*z*	*OCC*	*Biso.*
Nd	4e	0.25000	0.12164	0.00000	0.46	-0.76351
Y	4e	0.25000	0.12164	0.00000	0.04	-0.76351
Nb	4e	0.25000	0.64525	0.00000	0.5	-0.45242

O1	8f	0.03430	0.71966	0.21131	1.0	-1.48755
O2	8f	0.91186	0.45173	0.21261	1.0	-1.98655

Table.3 The bond strength for $(Nd_{1-x}Y_x)NbO_4$ (0.02≤x≤0.15) ceramics sintered at 1250 °C for 4h.

Bond type	Bond Strength					
	x=0.02	*x=0.04*	*x=0.06*	*x=0.08*	*x=0.10*	*x=0.15*
Nd/Y-O(1)^1×2	0.3753	0.3762	0.3782	0.4267	0.2305	0.2109
Nd/Y-O(1)^2×2	0.3270	0.3278	0.3293	0.3203	0.3252	0.3424
Nd/Y-O(2)^1×2	0.4350	0.4359	0.4378	0.4556	0.2426	0.2139
Nd/Y-O(2)^2×2	0.2678	0.2684	0.2697	0.2755	0.5205	0.5928
Nb-O(1)^1×2	0.9724	0.9744	0.9783	1.1458	1.2465	0.2427
Nb-O(1)^2×2	0.3871	0.3877	0.3890	0.3390	0.4259	0.4202
Nb-O(2) ×2	1.5918	1.5941	1.5996	1.6130	1.7139	1.8723
Total Nb-O	2.9513	2.9562	2.9669	3.0978	3.3863	3.5352

Table.4 Theoretical dielectric constant (ε_{rt}), corrected theoretical dielectric constant (ε_{rc}), the molecular polarizability (α_D) and coordination numbers (Z) for $(Nd_{1-x}Y_x)NbO_4$ (0.02≤x≤0.15) ceramics sintered at 1250 °C for 4h.

x value	*x=0.02*	*x=0.04*	*x=0.06*	*x=0.08*	*x=0.10*	*x=0.15*
Z	4	4	4	4	4	4
α_D	16.996	16.972	16.948	16.924	16.900	16.840
ε_{rt}	28.847	28.751	28.974	30.532	28.772	27.608
ε_{rc}	26.740	26.799	27.245	28.867	26.909	25.561

Table.5 Lattice energy for $(Nd_{1-x}Y_x)NbO_4$ ($0.02 \le x \le 0.15$) ceramics sintered at 1250 °C for 4h.

Bond type	Lattice Energy *U* (kJ/mol)					
	x=0.02	***x=0.04***	***x=0.06***	***x=0.08***	***x=0.10***	***x=0.15***
Nd/Y-O(1)^1×2	1463	1464	1465	1487	1437	1447
Nd/Y-O(1)^2×2	1438	1438	1439	1435	1377	1361
Nd/Y-O(2)^1×2	1406	1407	1408	1415	1439	1462
Nd/Y-O(2)^2×2	1324	1325	1326	1329	1310	1289
Nb-O(1)^1×2	7135	7136	7140	7306	7393	7389
Nb-O(1)^2×2	6203	6204	6207	6074	6293	6279
Nb-O(2) ×2	6912	6913	6916	6924	6981	7068
Total U_{Nd-O}	5631	5634	5638	5666	5563	5559

Table.6 The nonpolar covalence energy E_c^{μ} (kJ/mol), complete ionicity energy E_i^{μ} (kJ/mol), covalent blending coefficients t_c and ionic blending coefficients t_i for $(Nd_{0.92}Y_{0.08})NbO_4$ ceramics sintered at 1250 °C for 4h.

Bond type	E_c^{μ}	E_i^{μ}	t_c	t_i
Nd/Y-O(1)^1×2	213.95	568.91	0.6177	0.3823
Nd/Y-O(1)^2×2	204.71	545.31	0.6177	0.3823
Nd/Y-O(2)^1×2	216.12	575.70	0.6177	0.3823
Nd/Y-O(2)^2×2	200.02	532.82	0.6177	0.3823
Nb-O(1)^1×2	572.16	748.15	0.6917	0.3083
Nb-O(1)^2×2	448.48	586.43	0.6917	0.3083
Nb-O(2) ×2	612.67	801.12	0.6917	0.3083

Table.7 The bond energy for $(Nd_{1-x}Y_x)NbO_4$ ($0.02 \le x \le 0.15$) ceramics sintered at 1250 °C for 4h.

Bond type	Bond Energy E_B (kJ/mol)					
	x=0.02	*x=0.04*	*x=0.06*	*x=0.08*	*x=0.10*	*x=0.15*
Nd/Y-O(1)^1×2	336.14	338.67	341.30	350.02	320.47	321.06
Nd/Y-O(1)^2×2	329.09	331.57	334.11	334.91	337.88	345.91
Nd/Y-O(2)^1×2	343.86	346.43	349.06	353.58	363.25	376.39
Nd/Y-O(2)^2×2	319.13	321.52	324.00	327.24	323.01	321.76
Nb-O(1)^1×2	606.21	606.46	606.93	626.43	637.07	636.68
Nb-O(1)^2×2	504.22	504.37	504.70	491.01	513.93	512.55
Nb-O(2) ×2	669.00	669.19	669.65	670.78	678.96	691.07
E_B	3107.65	3118.21	3129.75	3153.97	3174.57	3205.42

Table.8 The relative density R.D. (%), dielectric constant ε_r, quality factor $Q \times f$ (GHz) and the temperature coefficient of resonant frequency τ_f (ppm/^{o}C) of $(Nd_{1-x}Y_x)NbO_4$ ($0.02 \le x \le 0.15$) ceramics sintered at 1250 °C for 4 h.

x value	*R.D.*	ε_r	$Q \times f$	τ_f
0.02	94.87	18.91	36700	-26.29
0.04	95.23	19.34	38700	-25.46
0.06	95.81	19.43	50800	-20.07
0.08	96.18	19.87	81100	-18.84
0.10	95.45	19.33	53300	-17.48
0.15	94.78	19.16	36600	-16.35

A table of contents entry

Phase composition, crystal structure and complex chemical bond theory investigated for the first time in the $(Nd_{1-x}Y_x)NbO_4$ system.